Polyhedron 29 (2010) 280–287

Contents lists available at ScienceDirect

Polyhedron

journal homepage: www.elsevier.com/locate/poly

Dependence of the product on the P–P ligand in reactions of [$RuCl_3$(NO)(P–P)] complexes (P–P = aromatic diphosphines) with 2-mercaptopyridine

Gustavo Von Poelhsitz [a,*], André L. Bogado [b], Luciano M. Lião [c], Antonio G. Ferreira [d], Eduardo E. Castellano [e], Javier Ellena [e], Alzir A. Batista [d]

[a] Departamento de Química, Universidade Federal de Goiás, Campus Catalão, CEP 75704-020, Catalão (GO), Brazil
[b] Faculdade de Ciências Integradas do Pontal, Universidade Federal de Uberlândia, CEP 38302-000, Ituiutaba (MG), Brazil
[c] Instituto de Química, Universidade Federal de Goiás, C.P. 131, CEP 74001-970, Goiânia (GO), Brazil
[d] Departamento de Química, Universidade Federal de São Carlos, C.P. 676, CEP 13565-905, São Carlos (SP), Brazil
[e] Instituto de Física de São Carlos, Universidade de São Paulo, C.P. 369, CEP 13560-970, São Carlos (SP), Brazil

ARTICLE INFO

Article history:
Available online 9 September 2009

Keywords:
Ruthenium nitrosyl complexes
Diphosphines
2-Mercaptopyridine
Dangling dppbO

ABSTRACT

This study presents the syntheses and characterization of 2-mercaptopyridine (pyS^-) complexes containing ruthenium(II) with the following general formula [$Ru(pyS)_2$(P–P)], P–P = (c-dppen) = *cis*-1,2-bis(diphenylphosphino)ethylene) **(1)**; (dppe) = 1,2-bis(diphenylphosphino)ethane **(2)**; (dppp) = 1,3-bis(diphenylphosphino)propane **(3)** and (dppb) = 1,4-bis(diphenylphosphino)butane **(4)**. The complexes were synthesized from the *mer*- or *fac*-[$RuCl_3$(NO)(P–P)] precursors in the presence of triethylamine in methanol solution with dependence of the product on the P–P ligand. The reaction of pyS^- with a ruthenium complex containing a bulky aromatic diphosphine dppb disclosed a major product with a dangling coordinated dppbO-P, the [$Ru(pyS)_2(NO)(\eta^1$-dppbO-P)]PF_6 **(5)**. In addition, this work also presents and discusses the spectroscopic and electrochemical behavior of **1**–**5,** and report the X-ray structures for **1** and **5**.

1. Introduction

Nitric oxide (NO) is relevant for many physiological processes, such as cytotoxicity, neural-transmission and blood pressure regulation, and its imbalance relates to diseases, for example cancer, epilepsy, diabetes and arthritis [1]. S-nitrosothiols (R-SNO) are believed to play an important role in storing, transporting, and releasing NO in the human body [1]. The ability of transition metal complexes to both scavenge and release NO has generated new interest in such complexes as potential metallopharmaceuticals [2]. As a non-innocent ligand that can be coordinated as NO^+, NO^0 or NO^-, depending on the nature of the metal center and on the coordination environment [3], nitric oxide promotes the formation of complexes with unique properties [3,4]. Many nitrosyl complexes have been utilized as metallodrugs and among them ruthenium complexes are of great interest [2,5,6]. Ruthenium has a high affinity for NO, and some complexes of this metal with coordinated NO have therapeutic uses in the treatment of sepsis and in the control of high blood pressure [2,7]. Considering the electrophilic character of the coordinated NO in a wide range of complexes, biological reducing agents, such as thiols, are able to reduce the NO group promoting its labilization [8,9]. In this sense it is interesting to study the reactions between nitrosyl complexes and ligands containing thiols residues, such as the complexes with general formula [Ru('$SpymMe_2$',–N,–S)('$SpymMe_2$',–S)(NO)(P–P)]$^+$, P–P = (dppe) or (c-dppen), '$SpymMe_2$',–N,–S = dimethylmercaptopyrimidine recently reported [10]. Ligands of the mercaptopyridine type and their complexes are currently being investigated as antiviral, antimetabolite and antitumor drugs as well as for their interesting photochemical properties [11–14]. These ligands are ubiquitous *S*, *N* donors that form a wide variety of complexes with different kinds of metals [15,16].

Herein are described the synthesis of mixed P–P and 2-mercaptopyridine complexes containing ruthenium with general formula [$Ru(pyS)_2$(P–P)], P–P = c-dppen **(1)**, dppe **(2)**, dppp **(3)** or dppb **(4)** and [$Ru(pyS)_2(NO)(\eta^1$-dppbO-P)]PF_6 **(5),** as well as a complete characterization, including spectroscopic, electrochemical behavior and elemental analysis. The X-ray crystals structures of the complexes **1** and **5** are also reported and discussed.

2. Experimental

2.1. Materials and instrumentation

All manipulations were carried out under Ar using standard Schlenk techniques. Reagent grade solvents were appropriately distilled and dried before use. $RuCl_3NO{\cdot}2H_2O$, *mer*-[$RuCl_3(H_2O)$

* Corresponding author. Tel.: +55 64 34415334; fax: +55 64 34415336.
E-mail address: gustvon@catalao.ufg.br (G. Von Poelhsitz).

0277-5387/$ - see front matter © 2009 Elsevier Ltd. All rights reserved.
doi:10.1016/j.poly.2009.09.004

(dppb)], *mer*-[$RuCl_3$(NO)(dppb)] and *fac*-[$RuCl_3$(NO)(P–P)], P–P = c-dppen, dppe, dppp and dppb, were prepared following the procedures described in the literature in earlier works from this group [17–19]. NMR spectra were recorded on a Bruker DRX 400 – 9.4 T spectrometer at 298 K using a 5 mm direct probehead. The spectra were obtained at 400.21 MHz for ^{1}H, 100.05 MHz for ^{13}C and 162 MHz for ^{31}P. ^{1}H and ^{13}C shifts were recorded using TMS as internal standard. ^{31}P shifts were referenced to H_3PO_4, 85%. The proton phosphorus decoupled $^1H\{^{31}P\}$ NMR experiment was performed using a relaxation delay of 1.0 s, pulse width 3.5 μs for 30°, sweep width of 8116 Hz, acquisition time 4.03 s and 16 transients for each spectrum. IR spectra were recorded on a Bomem Michelson FT MB-102 spectrophotometer as CsI pellets. UV–Vis spectra were recorded on a Varian-Cary 500 spectrometer using quartz cells and are presented as λ_{max} or shoulder (sh) (nm)/ε_{max} ($M^{-1}\,cm^{-1}$). Cyclic voltammetric measurements were recorded with a potentiostat BAS-100 B. A three-compartment cell was used with an Ag/AgCl reference electrode separated from a Pt disk working electrode and Pt disk auxiliary electrode. Freshly distilled dichloromethane was used as solvent in these measurements and $Bu_4N^+ClO_4$ (TBAP – Fluka Purum) was used as supporting electrolyte. Solutions containing 10^{-3} mol L^{-1} analyte (0.1 mol L^{-1} electrolyte) were deoxygenated for 5 min by a vigorous Ar purge. All $E_{1/2}$ values were calculated from $(E_{pa} + E_{pc})/2$ at a scan rate of 100 mV s^{-1}. Elemental analyses were performed by Microanalytical Laboratory of Universidade Federal de São Carlos on a FISONS CHNS, mod. EA-1108. The ESI analyses were done in a Micromass, triple-quadrupole, ESI/APCI spectrometer utilizing CH_2Cl_2 as solvent.

2.2. Synthesis

2.2.1. [Ru(pyS)$_2$(c-dppen)] **(1)**

A solution of 2-mercaptopyridine (0.48 mmol, 54.0 mg) in methanol (5 mL) with triethylamine (0.96 mmol, 0.13 mL) was transferred via cannula in a Schlenk flask containing a methanolic suspension (25 mL) of the *fac*-[$RuCl_3$(NO)(c-dppen)] (0.16 mmol, 100 mg). The mixture was heated under reflux for 12 h providing a yellow precipitate that was collected by filtration, washed with methanol and ether, and dried under vacuum. Same results can be achieved without refluxing if time reaction within 24 h. *Anal.* Calc. for $C_{36}H_{30}P_2N_2S_2Ru$: C, 60.24; H, 4.21; N, 3.90. Found: C, 60.43; H, 4.42; N, 3.82%. Yield: 62.0 mg (55%). UV–Vis (CH_2Cl_2) λ_{max}, nm (log ε, $mol^{-1}\,dm^3\,cm^{-1}$): 311 (4.13), 390 (3.45), 440 (2.94). $^{31}P\{^1H\}$ NMR ($CDCl_3$, δ, ppm): 78.4 (s). ^{1}H NMR ($CDCl_3$, δ, ppm): 6.28 (dt, J = 8.1; 1.0 Hz, 2H, H3-pyS), 6.44 (ddt, J = 7.3; 5.4; 1.2 Hz, 2H, H5-pyS), 6.95 (ddd, J = 8.1; 7.3; 1.8 Hz, 2H, H4-pyS), 7.00–7.30 (m, 20H, Ph), 7.66 (ddd, J = 59.8; 37.8; 8.2 Hz, 2H, CH=CH, ^{1}H and ^{31}P coupling), 8.02–8.06 (m, 2H, H6-pyS). ^{13}C NMR ($CDCl_3$, δ, ppm): 115.6 (C3-pyS), 124.9 (C5-pyS), 127.5–134.5 (Ph), 133.9 (C4-pyS), 147.9 (C6-pyS), 149.9 (CH=CH), 181.7 (C2-pyS). ^{1}H NMR (CD_2Cl_2, δ, ppm): 6.36 (dt, J = 8.1; 1.0 Hz, 2H, H3-pyS), 6.60 (ddt, J = 7.3; 5.4; 1.2 Hz, 2H, H5-pyS), 7.11 (ddd, J = 8.1; 7.3; 1.8 Hz, 2H, H4-pyS), 7.13–7.44 (m, 20H, Ph), 7.80 (ddd, J = 59.8; 37.8; 8.2 Hz, 2H, CH=CH, ^{1}H and ^{31}P coupling), 8.15–8,19 (m, 2H, H6-pyS). $^1H\{^{31}P\}$ NMR (CD_2Cl_2, δ, ppm): 6.36 (dt, J = 8.1; 1.0 Hz, 2H, H3-pyS), 6.60 (ddd, J = 7.3; 5.4; 1.2 Hz, 2H, H5-pyS), 7.11 (ddd, J = 8.1; 7.3; 1.8 Hz, 2H, H4-pyS), 7.13–7.41 (m, 20H, Ph), 7.79 (s, 2H, CH=CH, no ^{1}H and ^{31}P coupling), 8.17 (ddd, J = 5.4; 1.8; 1.0, 2H, H6-pyS). IR (CsI, cm^{-1}): νCN = 1576 m, νCS = 1135 s, νP–C(ϕ) = 1094 m; also 3071 w, 3047 w, 3014 w, 3002 w, 2923 w, 1544 m, 1480 m, 1436 m, 1419 s, 747 s, 734 m, 697 m, 529 m, 417 w, 377 w.

2.2.2. [Ru(pyS)$_2$(P–P)], P–P = dppe **(2)**, dppp **(3)**

Same procedure described for **1** utilizing the corresponding precursor complexes.

(**2**) Anal. Calc. (%) for $C_{36}H_{32}P_2N_2S_2Ru$: C, 60.06; H, 4.48; N, 3.89. Found: C, 59.88; H, 4.65; N, 3.78%. Yield: 66.0 mg (58%). UV–Vis (CH_2Cl_2) λ_{max}, nm (log ε, $mol^{-1}\,dm^3\,cm^{-1}$): 318 (4.13), 392 (3.38), 445 (2.83). $^{31}P\{^1H\}$ NMR (δ, ppm): 74.0 (s).

(**3**) Anal. Calc. for $C_{37}H_{34}P_2N_2S_2Ru$: C, 60.56; H, 4.67; N, 3.82. Found: C, 60.85; H, 4.32; N, 4.07%. Yield: 60.0 mg (53%). UV–Vis (CH_2Cl_2) λ_{max}, nm (log ε, $mol^{-1}\,dm^3\,cm^{-1}$): 322 (4.01), 390 (3.28), 441 (2.84). $^{31}P\{^1H\}$ NMR (δ, ppm): 42.1 (s).

2.2.3. [Ru(pyS)$_2$(dppb)] **(4)** and [Ru(pyS)$_2$(NO)(^{1}-dpppbO-P)]PF_6 **(5)**

The precursor *mer*-[$RuCl_3$(NO)(dppb)] (0.15 mmol, 100.0 mg) was reacted with excess of the 2-mercaptopyridine ligand (0.48 mmol, 54.0 mg) in methanol (20 mL) within 24 h. The ligand was previously deprotonated with triethylamine (0.96 mmol, 0.13 mL) in methanol and added via cannula over the precursor solution. After the reaction time a small amount of a yellow powder was filtered off and identified as **4**, and the red solution obtained was concentrated to ca. 5 mL and NH_4PF_6 was added (0.20 mmol, 32.6 mg). This solution was maintained in the freezer at −10 °C and after 48 h a red powder identified as **5** was recovered. The same reaction described above but utilizing the *fac* isomer instead the *mer* resulted in the formation of the complex **5** as the sole product.

(**4**) Anal. Calc. for $C_{38}H_{36}P_2N_2S_2Ru$: C, 61.03; H, 4.85; N, 3.75. Found: C, 61.32; H, 4.63; N, 3.65%. Yield: 16.0 mg (14%). UV–Vis (CH_2Cl_2) λ_{max}, nm (log ε, $mol^{-1}\,dm^3\,cm^{-1}$): 324 (4.00), 396 (3.15), 446 (2.69). $^{31}P\{^1H\}$ NMR (δ, ppm): 49.1 (s).

(5) *Anal.* Calc. (%) for $C_{38}H_{36}P_2N_3O_2S_2RuPF_6$: C, 48.60; H, 3.87; N, 4.48. Found: C, 48.30; H, 3.89; N, 4.76%. Yield: 76.0 mg (54%). UV–Vis (CH_2Cl_2) λ_{max}, nm (log ε, $mol^{-1}\,dm^3\,cm^{-1}$): 260 (4.69), 323 (3.85), 424 (2.75). $^{31}P\{^1H\}$ NMR (δ, ppm): 31.4 (s); 35.9 (s). ^{1}H NMR ($CDCl_3$, δ, ppm): 2.32 (dt, J = 11.3; 8.1, 4H, CH_2), 2.56–2.47 (m, 2H, CH_2), 2.93–2.84 (m, 2H, CH_2), 6.51 (ddd, J = 7.5; 5.8; 1.2, 2H, H5-pyS), 6.82 (dt, J = 8.2; 1.0, 2H, H3-pyS), 7.05 (ddt, J = 5.8; 1.4; 1.2, 2H, H4-pyS), 7.11 (dd, J = 8.2; 1.0, 2H, Ph), 7.29–7.38 (m, 4H, Ph), 7.40–7.46 (m, 4H, Ph), 7.70 (ddd, J = 8.2; 7.5; 1.6, 2H, Ph), 7.75–7.81 (m, 8H, Ph), 8.42–8.45 (m, 2H, H6-pyS). ^{13}C NMR ($CDCl_3$, δ, ppm): 22.7 (CH_2), 24.2 (CH_2), 26.5 (CH_2), 28.5 (CH_2), 119.5 and 120.2 (C3-pyS), 125.7-133.4 (Ph), 127.4 and 127.5 (C5-pyS), 139.6 and 140.3 (C4-pyS), 144.2 and 145.7 (C6-pyS), 173.6 and 178.4 (C2-pyS). ES mass spectrum (CH_2Cl_2, m/z): 795, $[M-PF_6+H]^+$. IR (CsI, cm^{-1}): νNO = 1858 s, νCN = 1590 m; 1585 m, νP=O = 1187 m, νCS = 1144 w; 1139 w, νP–C(ϕ) = 1100 m; also 3105 w, 3058 w, 3018 w, 3012 w, 2931 w, 2904 w, 2890 w, 2869 w, 2829 w, 1557 m, 1487 w, 1445 s, 1437 s, 1429 s, 836 s, 759 s, 740 s, 719 s, 700 s, 690 s, 596 w, 549 s, 518 m, 507 m, 492 m, 425 w, 365 w.

Observation: the characterization data (^{1}H and ^{13}C NMR, IR and UV–Vis spectroscopies, and elemental analysis) for complexes **2–4** were previously published by Lobana et al. [20] and will not be described here again. Our data are in agreement with the previously reported such a way we will only discuss the data not published, mainly the $^{31}P\{^1H\}$ NMR.

2.3. X-ray structural determinations

Suitable crystals of **1** were grown by careful addition of diethyl ether into dichloromethane solutions at room temperature. Red crystals of **5** were obtained by cooling the reactional mixture of the respective compound in the presence of PF_6^- anion. The crystals were mounted on an Enraf-Nonius Kappa-CCD diffractometer with graphite monochromated Mo Kα (λ = 0.71073 Å) radiation. The final unit cell parameters were based on all reflections. Data collections were made using the COLLECT program [21]; integration and scaling of the reflections were performed with the HKL Denzo-Scalepack system of programs [22]. Absorption corrections

were carried out using the "semiempirical" [22] and "multi-scan" [23] methods, respectively, for **1** and **5**. The structures were solved by direct methods with SHELXS-97 [24]. The model was refined by full-matrix least squares on F^2 by means of SHELXL-97 [25]. All hydrogen atoms were stereochemically positioned and refined with the ridging model. Figs. 1 and 2 were prepared using ORTEP-3 for windows [26]. Hydrogen atoms of the aromatic rings and CH and CH_2 were set isotropic with a thermal parameter 20% greater

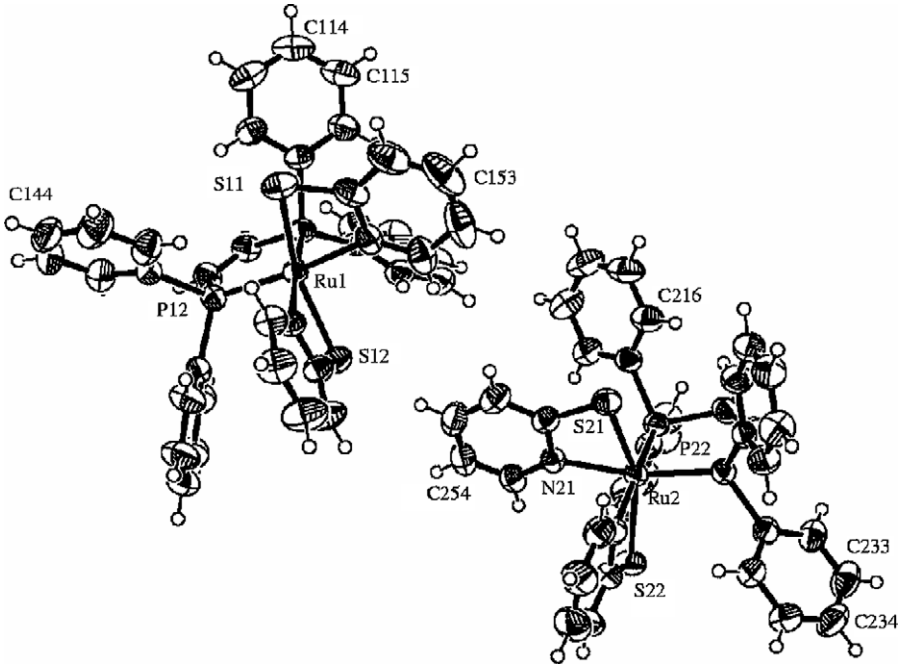

Fig. 1. ORTEP view of **Δ** and **Λ**-[Ru(pyS)$_2$(c-dppen)] (**1**) showing the atoms labeling and the 50% probability ellipsoids. Bond Lengths average from Δ and Λ isomers (Å): Ru–N(2) 2.124(3), Ru–N(1) 2.141(4), Ru–P(1) 2.2571(10), Ru–P(2) 2.2603(11), Ru–S(1) 2.4278(11), Ru–S(2) 2.4313(11), C(1)–C(2) 1.322(7). Bond angles average from Δ and Λ isomers (°)**:** N(2)–Ru–N(1) 85.13(13), N(2)–Ru–P(1) 170.60(9), N(1)–Ru–P(1) 98.15(9), N(2)–Ru–P(2) 93.72(10), N(1)–Ru–P(2) 172.23(9), P(1)–Ru–P(2) 84.20(4), N(2)–Ru–S(1) 92.32(9), N(1)–Ru–S(1) 67.44(9), P(1)–Ru–S(1) 97.07(4), P(2)–Ru–S(1) 104.97(4), N(2)–Ru–S(2) 67.35(9), N(1)–Ru–S(2) 93.69(10), P(1)–Ru–S(2) 103.55(4), P(2)–Ru–S(2) 92.95(4).

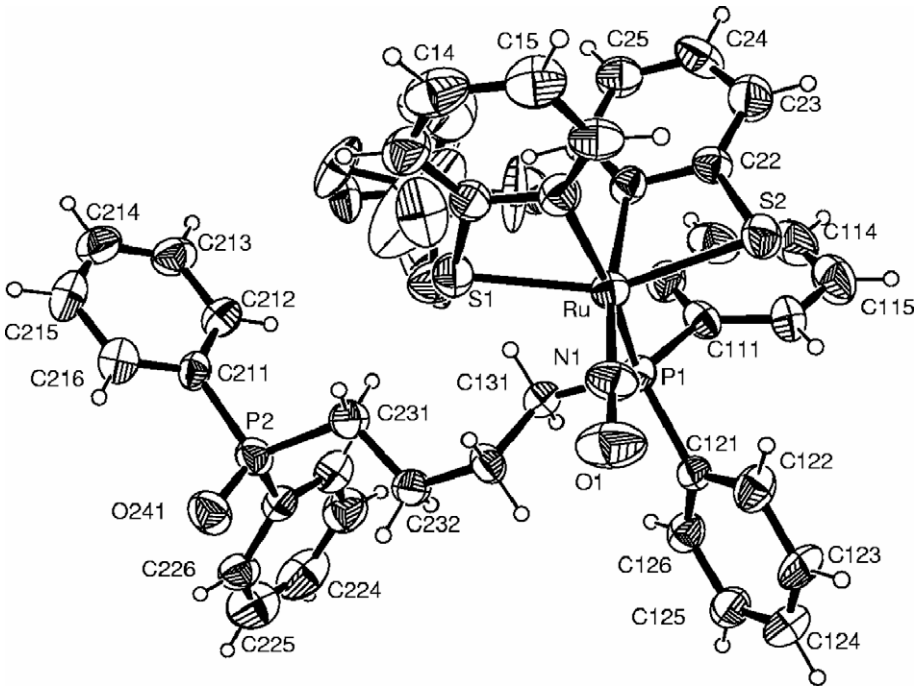

Fig. 2. ORTEP view of [Ru(pyS)$_2$(NO)(dppbO-P)]PF$_6$ (**5**) showing the atoms labeling and the 50% probability ellipsoids. Bond lengths (Å): Ru–N(1) 1.714(9), Ru–N(21) 2.074(8), Ru–N(11) 2.140(9), Ru–P(1) 2.383(3), Ru–S(1) 2.407(3), Ru–S(2) 2.418(3), O(1)–N(1) 1.154(10), P(2)–O(241) 1.469(7). Bond angles (°): N(1)–Ru–N(21) 171.3(4), N(1)–Ru–N(11) 95.7(4), N(21)–Ru–N(11) 86.7(3), N(1)–Ru–P(1) 93.5(3), N(21)–Ru–P(1) 85.5(2), N(11)–Ru–P(1) 166.9(2), N(1)–Ru–S(1) 97.0(4), O(1)–N(1)–Ru 178.5(11), N(21)–Ru–S(1) 91.6(2), N(11)–Ru–S(1) 68.2(3), P(1)–Ru–S(1) 101.51(11), N(1)–Ru–S(2) 102.9(4), N(21)–Ru–S(2) 68.6(3), N(11)–Ru–S(2) 94.5(3), P(1)–Ru–S(2) 92.49(11), S(1)–Ru–S(2) 154.88(10).

Table 1
Summary of X-ray parameters for the complexes **1** and **5**.

	1	**5**
Empirical formula	$C_{36}H_{30}N_2S_2P_2Ru{\cdot}CH_3OH$	$C_{38}H_{36}N_3O_2P_2S_2Ru{\cdot}PF_6$
M	749.79	938.80
Space group	$P\bar{1}$, triclinic	$Pna2_1$, orthorhombic
a (Å)	11.5100(3)	13.6400(5)
b (Å)	12.2800(4)	26.2180(5)
c (Å)	12.3200(4)	11.6330(11)
α (°)	79.087(2)	
β (°)	84.865(2)	
γ (°)	87.970(2)	
U (Å^3)	1702.69(9)	4160.1(4)
Z	2	4
D_c (Mg m^{-3})	1.462	1.499
T (K)	293	293
F(0 0 0)	768	1904
μ (mm^{-1})	0.710	0.656
2θ limit (°)	1.69–27.03	2.43–25.0
h, *k*, *l Ranges*	−13 to 13, −14 to 14, −14 to 14	−15 to 15, −30 to 31, −13 to 13
Reflections collected	10 867	20 059
Unique reflections (R_{int})	6025 (0.0165)	6892 (0.1449)
Final *R* indices	*R* = 0.0364, *R*′ = 0.1232	*R* = 0.0571, *R*′ = 0.1172
(All data)	*R* = 0.0471, *R*′ = 0.1477	*R* = 0.1317, *R*′ = 0.1585
Goodness-of-fit, *S*	1.300	1.201
No. of parameters	6025	549
Peak and hole (e Å^{-3})	0.679 and −1.468	0.539 and −0.842

than the equivalent isotropic displacement parameter of the atom to which each one is bonded. The data collections and experimental details are summarized in Table 1.

3. Results and discussion

3.1. Synthesis and structural characterization

Previous studies in our laboratory showed that the products of the reactions of complexes with general formula *mer*- or *fac*-[$RuCl_3$(NO)(P–P)], P–P = aromatic diphosphines, with the 2-mercaptopyridine (pyS^-), are dependent of the P–P ligand [27,28]. For dppm (bis(diphenylphosphine)methane) it was found that selective oxidation of one phosphorus atom produces a nitrosyl complex containing a dangling dppmO as ligand, the [Ru(pyS)$_2$(NO)(η^1-dppmO-P)]PF_6 [27]. However, with dppe or dppp the products were identified by spectroscopic techniques (^{31}P NMR, IR and UV–Vis) and elemental analysis as the thiolate derivatives [Ru(pyS)$_2$(P–P)], which have previously been reported by Lobana et al. [20,29]. In the present work the [Ru(pyS)$_2$(P–P)] complexes were obtained from *mer* or *fac*-[$RuCl_3$(NO)(P–P)] precursors whereas in the previously reported studies the compounds were obtained from the addition of pyS^- to *cis*-[$RuCl_2$(P–P)$_2$] complexes with one diphosphine displacement (see Scheme 1). In previous studies we noticed a partial oxidation of the [Ru(pyS)$_2$(P–P)] complexes, P–P = dppe or dppp, when in solution and exposed to air, producing crystals with formulae [Ru($pySO_2$)$_{0.33}$(pyS)$_{1.67}$(dppe)] and [Ru($pySO_2$)$_{0.355}$(pyS)$_{1.645}$(dppp)][28], as expected from the well known sulfur-centered reactivity of transition metal thiolates with dioxygen to produce sulfur oxygenates [30,31].

In order to better explore this difference in reactivity, reactions of the complexes *fac*-[$RuCl_3$(NO)(c-dppen)] and *mer*-[$RuCl_3$(NO)(dppb)] were carried out with the 2-pyS^- ligand. In these reactions it distinct products depending on the P–P ligand were obtained, the [Ru(pyS)$_2$(c-dppen)] **(1)** and the [Ru(pyS)$_2$(NO)

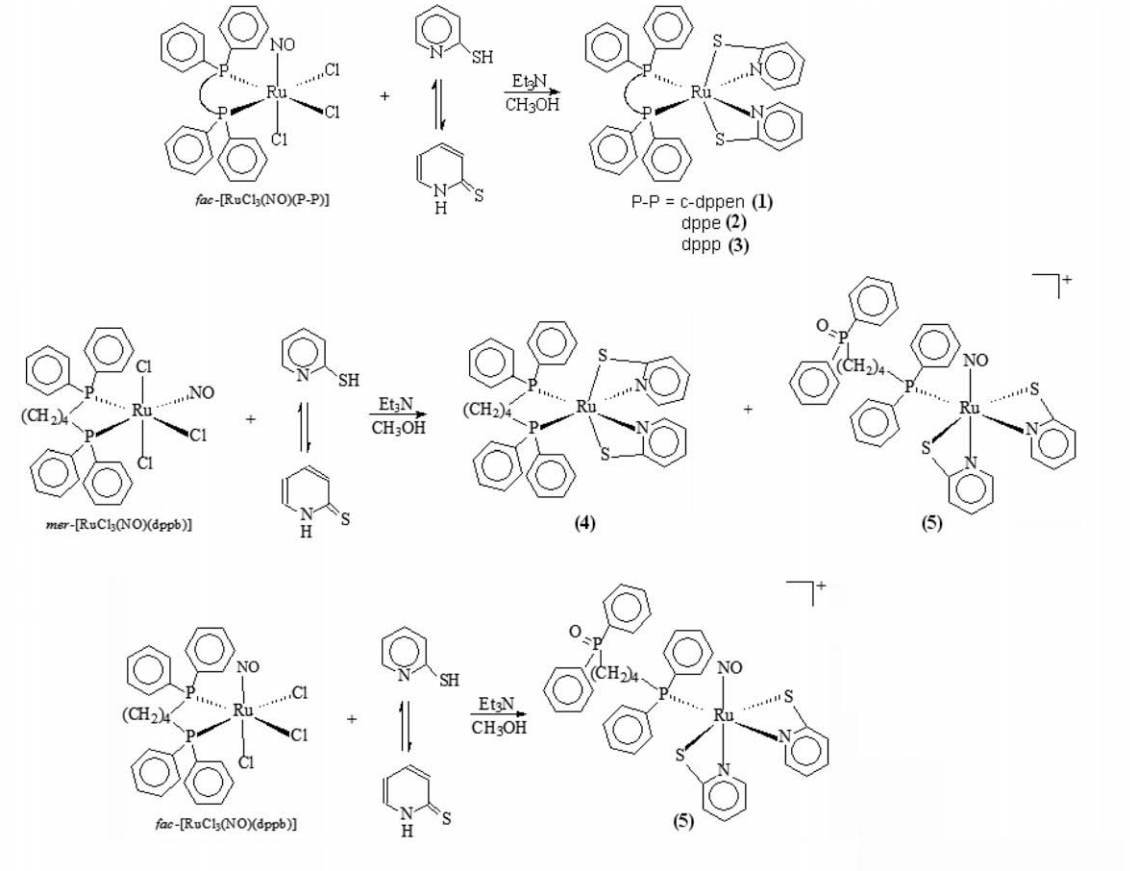

Scheme 1. Ruthenium nitrosyl complexes as starting material to prepare bis-mercaptopyridine derivatives.

(dppbO-P)]PF_6 **(5)**. Interestingly, complex **5** contains a dangling coordinated dppbO-P (see Scheme 1). Bis-phosphino monoxides such as dppbO are hemilabile ligands due to the presence of the soft (P) and hard (O) Lewis base centers on the same molecule [32]. These molecules are very interesting ligands for the preparation of metal complexes for application in homogeneous catalysis [32].

The structures of **1** and **5** were determined by the X-ray diffraction method. The ORTEP view showing the atoms labeling and the 50% probability ellipsoids are presented in Figs. 1 and 2, and the bond lengths and angles selected are described in the caption. The structures adopt a six-coordinated structure with the thiolate-sulfur donor atoms of two pyS^- ligands occupying *trans* position in relation to each other. In complex **1** the coordination sphere is completed with a chelating c-dppen diphosphine with P *trans* N, therefore there is a $N_2P_2S_2$ set of donor atoms. Complex **1** crystallized as a racemate with no significative differences in bond lengths and angles between the two enantiomers Δ and Λ-[Ru($pyS)_2$(c-dppen)] (see Fig. 1). In **5** a dangling dppb-O and a NO molecule, both *trans* to the N of pyS ligands, complete the coordination sphere. In the structures depicted here distortions from an ideal octahedral geometry arise from the small bite angles of pyS^- (N–Ru–S = 67.34 (7) and 67.66 (7)), respectively, for **1** and **5**. The 'pyS' ligands in **1** have C–S bond distances of 1.762(10) and 1.765(9) Å, which are significantly longer than the C=S double bond distance of 1.62 Å, but shorter than a C–S single bond distance of 1.81 Å [33], suggesting that it has a partially double bound character [34]. The coordination of 2-pyS promotes some variations on the ligand dimensions [35]. In the pyridine-2-thionate anion the exocyclic thione (>C=S) distance is increased from 1.695(2) to 1.74 and 1.75 Å (av.), respectively, for **1** and **5**. The thioamide distance C–N decreases slightly, from 1.356(3) to 1.33 Å (av.) for both **1** and **5**, as does the N–C–S angle, which decreases from 120.6(1)° to 109.8 and 110.4° (av.), for **1** and **5,** respectively. All the observed changes in the pyS^- dimensions are in agreement with the shift of π-electron density to the amide (C–N) portion of the thioamide group, as well as with the concentration of the negative charge on the sulfur atom of the anion and with the enhancement of the thionate character of this ligand [15]. The observed distances related to the ruthenium center in **1** are close to that encountered for the dppe and dppp analogous [28,36]. The structure of **5** shows a nearly linear Ru–N–O angle [174.2(7)°] and an N–O distance of 1.154(10) Å, both indicating a {Ru^{II}–NO^+} type complex [27,37], as is also indicated by the IR spectrum. The Ru–S distances of nearly 2.40 Å are essentially identical to those observed in other complexes containing 'pyS^-' ligands [27,38]. The Ru–N (pyS^- ligand) distance of N *trans*-NO of 2.080(7) Å is slightly shorter than the N *trans*-P of 2.142(7) Å, which is probably due the fact that the NO acting as a strong π-acid reduces the Ru–N distance [39].

In order to evaluate the NO^+ character of the complex **5**, a reaction with the azide nucleophile was performed [40]. The ^{31}P NMR and IR data did not show any difference from that of the precursor complex indicating that the coordinated NO, in this case, is not sufficiently positive to be susceptible to nucleophilic attacks. The same was observed for the analogous [Ru($pyS)_2$(NO)(η^1-dppmO)]PF_6 [27].

3.2. UV–Vis studies

Electronic spectra of complexes **1–4** are dominated by an intense intraligand ($\pi \rightarrow \pi^*$ C–S) absorption band. This band occurs in higher energy than that observed for the free ligand, since the C=S bond order is lower with the sulfur coordination. The energy of this band was 311 nm for **1** whereas for **2–4** it was in the range 318–324 nm. This difference reflects the greater electronic delocalization of the c-dppen diphosphine when compared to the others, in such a way that the sulfur atom donates more electronic density to the ruthenium in **1** and its $\pi \rightarrow \pi^*$ transition is displaced to higher energy. It is interesting to mention that the strong bands for $\pi \rightarrow \pi^*$ transitions of the diphosphines ligands presented in the nitrosyl precursors (around 260 nm) are absent in these derivatives. The presence of a π acceptor ligand *trans* positioned (N of 2-pyS) justifies this observation, since that the competition for electronic density between the phosphorus and the nitrogen atoms makes the electronic density around the phosphorus smaller. Analyzing the spectrum of the nitrosyl derivative **5** we clearly noticed three absorption bands. The most energetic of them arises around 250 nm and can be attributed to the $\pi \rightarrow \pi^*$ intraligand diphosphine absorption bands due to the very high ε value. Still in the ultraviolet region, a band at 323 nm was observed, similarly to **1–4** complexes, in such a way that it is attributed to the pyridinic ligand as carried out in the earlier complexes. In the visible region there is a band at 424 nm which probably arises from a d–d transition due to the ε value of 500 M^{-1} L cm^{-1}. The electronic spectrum of complex **5** is very similar to the previously reported analogous [Ru($pyS)_2$(NO)(η^1-dppmO-*P*)]PF_6 [27].

3.3. Infrared studies

The IR spectra for complexes **1–4** are very similar to each other and are characterized by the typical vibrational modes of the aromatic diphosphines and the 2-pyS^- ligand [20,41]. For the nitrosyl complex **5,** an intense *ν*NO band at 1858 cm^{-1}, which is typical of a nitrosonium ligand bonded linearly to ruthenium, was observed [42,43]. Since the two coordinated 'pyS^-' ligands are not equivalent, the IR spectrum of the complex shows a larger number of vibrational modes from this ligand than in the spectrum of the [Ru($pyS)_2$(P–P)] species[20]. The presence of a medium intensity band at 1187 cm^{-1} is characteristic of *ν*P=O. This value is similar to the observed values for other ruthenium complexes containing an oxidized dangling phosphorus [28,44]. For association purposes, when the dppbO is bidentate through P and O atoms, the *ν*P=O decreases from 1187 to 1120 cm^{-1} as observed for the complexes [$RuCl_2$(η^2-dppbO)(N–N)], N–N = bipy or phen [45].

3.4. Electrochemical studies

The results of the cyclic voltammetric measurements for the complexes **1–5** in CH_2Cl_2 solutions at room temperature are presented in Table 2. In the case of complexes **1–4** a reversible process is observed with an $E_{1/2}$ value in the range of 0.33 to 0.41 V. The ratio between the anodic and cathodic half-wave peak currents is close to unity, attesting to the reversible character of the oxidation process. The difference between the values of the anodic and cathodic peak potentials exceeds the theoretical value of 59 mV for one-electron process, but such deviations are typical of reversible Ru^{III}/Ru^{II} pairs in nonaqueous media. The differences in $E_{1/2}$ values among complexes **1–4** are related to the ability of electronic delocalization from the diphosphines, thus the c-dppen, which has

Table 2
Cyclic voltammetric and $^{31}P\{^1H\}$ NMR data for complexes **1–5**.

Complex	$E_{1/2}$ (V)	ΔE ($E_a - E_c$) (V)	$^{31}P\{^1H\}$ NMR – δ ppm (m)
1	0.41	0.15	78.4 (s)
2	0.35	0.15	74.0 (s)
3	0.33	0.14	42.1 (s)
4	0.34	0.16	49.1 (s)
5	−0.39	0.14	31.4 (s) P^V; 35.9 (s) P^{III}
Free dppbO [32]			31.3 (s) P^V; −16.2 (s) P^{III}

δ, chemical shift, (*m*), multiplicity, (s), singlet.

a double bond at the bridge between P atoms, helps to better stabilize the metal center, increasing its redox potential.

As expected, the nitrosyl complex **5** showed a different behavior from the complexes **1–4**. **C**omplex **5** has a strong π-acceptor ligand such as NO, which stabilizes the ruthenium (II) oxidation state, providing an electrochemical process at the NO^+ group [46]. The electrochemical behavior of **5** (see Fig. 3) is similar to that observed for other nitrosyl complexes described in the literature, with two successive reduction waves centered at the coordinated nitrosyl [27,46,47].

The first process at −0.39 V is reversible, corresponding to the reduction of $[Ru(pyS)_2(NO)(dppbO\text{-}P)]^+$ to $[Ru(pyS)_2(NO)(dppbO\text{-}P)]^0$ and the more cathodic wave (quasi-reversible) at −1.15 V corresponds to the reduction of $[Ru(pyS)_2\text{-}(NO)(dppbO\text{-}P)]^0$ to $[Ru(pyS)_2(NO)(dppbO\text{-}P)]^-$. A similar behavior was observed for the $[Ru(Cp)(P\text{–}P)(NO)]^{2+}$ series, P–P = dppe, dppm or dmpe [1,2-bis(dimethylphosphine)ethane], which present two reversible waves shifted to more anodic potentials when compared with **5** [48]. After the second reduction wave, a new anodic peak appears close to 0.90 V. However, no additional study was carried out to identify such species. The analogous with dppmO showed a very similar behavior but with the first reversible process slightly displaced to cathodic potential and with no additional waves after the second reduction. In the utilized experimental condition the Fc/Fc^+ pair is shown at $E_{1/2}$ = +0.43 V. The reversible one-electron reduction process centered at the coordinated NO observed for **5** indicates a great stability of the reduced species promoted by the electron acceptor characteristic of the phosphorus and 'pyS' ligands that helps the distribution of electronic density added with the reduction.

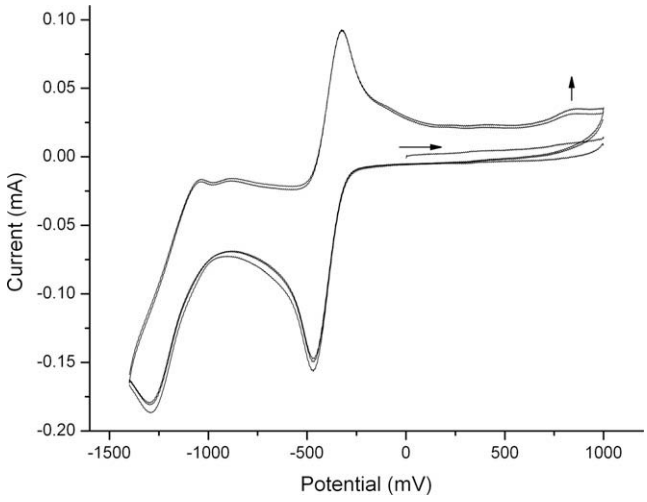

Fig. 3. Cyclic voltammogram of **5** in CH_2Cl_2 (TBAP – 100 mV s^{-1}).

3.5. NMR characterization

As shown in Table 2, complexes **1–4** showed one singlet signal in the $^{31}P\{^1H\}$ NMR spectra, indicating the magnetic equivalence of the phosphorus atoms and consequently the *trans* configuration for these complexes. Considering the variation of chemical shift, it can be noticed that the protection order is in agreement with the delta ring effect in which the five membered chelates (dppe and c-dppen) are down field shifted, while the six and seven ones show variable behavior. The c-dppen derivative shows an additional effect of electronic delocalization (the double bound), making the phosphorus more deshielded than the dppe one. The same order has been observed in the series $[Pd(S_2CNEt_2)(P\text{–}P)]^+$ [49], *trans*-$[RuCl_2(P\text{–}P)_2]$ [50] and *fac*-$[RuCl_3(NO)(P\text{–}P)]$ [17], as ascribed in the literature.

The nitrosyl derivative **5** presents a different characteristic from that aforementioned; one of the phosphorus is non-coordinated and oxidized. Therefore, two singlet signals for this compound can be observed, as shown in Fig. 4. For the dppm analogous, previously published, two doublets were observed [27]. Considering that the coupling between phosphorus in these complexes will happen just through chemical bonding instead of through *d* orbitals from metallic center plus chemical bonding contributions, it is possible to understand the small value of the coupling constant in **5** and, consequently, the observation of singlet signals instead of doublets. On the other hand, when the aliphatic group contains only a CH_2 between phosphorus the P–P scalar coupling is observed, as is the case of the $[Ru(pyS)_2(NO)(dppmO\text{-}P)]^+$ complex [27]. The more shielded signal is attributed to the oxidized phosphorus due to the almost coincidental signals of the complexes and of the dioxidized free phosphine. There are some examples of complexes with a chelated dppbO, as the $[RuCl_2(\eta^2\text{-dppbO})(bipy)]$ [45], where two singlets appeared at 32.2 and 53.4 ppm, respectively, corresponding to the P^V and P^{III} oxidations state.

The ^1H NMR spectrum of **1** presents an AA'XX' system for the CH=CH protons of the c-dppen ligand. This system caused by coupling between ^1H and ^{31}P generates a second-order pattern as shown in Fig. 5. The multiplicity rules between $^{31}P\text{–}^1H$ and $^1H\text{–}^1H$ are the same, and a coupling constant could be observed up to four bonds. A similar behavior was observed for the complexes $[ReOCl_3(c\text{-dppen})]$ and $[ReOCl_2(OEt)(c\text{-dppen})]$ described in the literature [51], for these cases a simulation was carried out and a perfect fit was obtained. In our case, a different approach to study this second-order system was chosen. We performed a

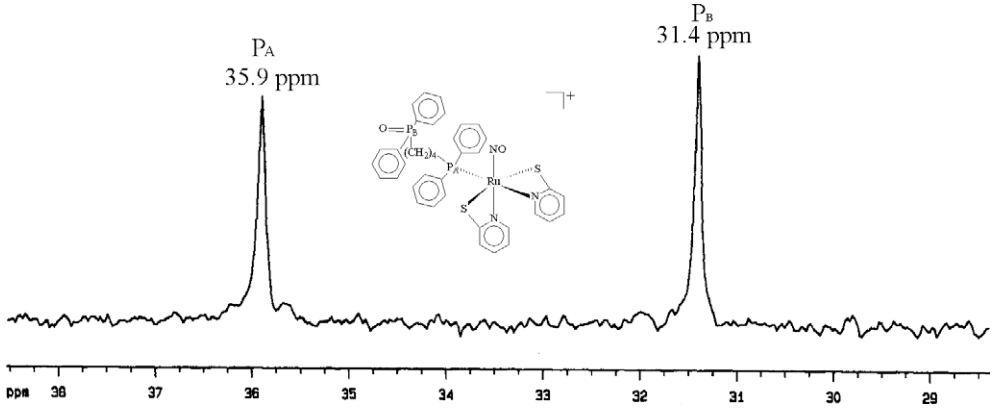

Fig. 4. $^{31}P\{^1H\}$ spectrum of **5** in $CDCl_3$ solution at room temperature.

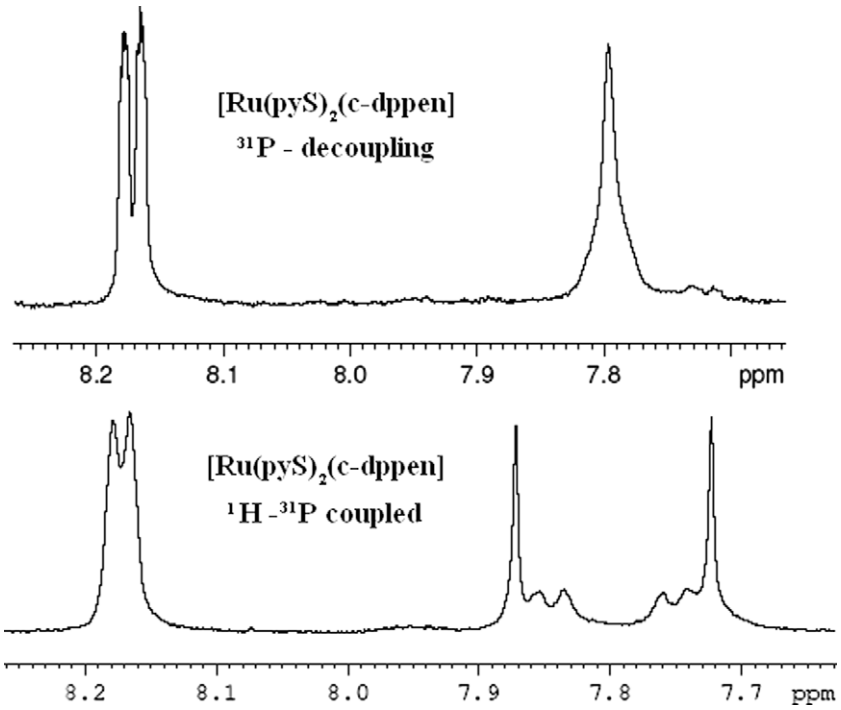

Fig. 5. ^{1}H and $^{1}H\{^{31}P\}$ NMR spectra of **1** in CD_2Cl_2 solution at room temperature.

$^{1}H\{^{31}P\}$ NMR experiment, in such a way that the coupling constants of ^{1}H with ^{31}P were eliminated. The obtained spectrum shown in Fig. 5 presented a singlet signal instead of the second-order pattern signal for the CH═CH group, indicating the magnetic equivalence of these protons. The other signals for the c-dppen ligand appeared as multiplets in the 7.13–7.41 ppm range. The two pyS^{-} ligands coordinated to ruthenium are equivalent and their four hydrogens appeared as a deshielded doublet of a doublet of doublet at 8.17, two others at 7.11 and 6.60 and a doublet of triplet at 6.36 ppm. These chemical shift values are very similar to those found for the analogous $[Ru(pyS)_2(P–P)]$ previously published [36].

4. Conclusions

This work presented a study on the dependence of the product on the P–P ligand in the reactions of $[RuCl_3(NO)(P–P)]$ complexes (P–P = aromatic diphosphines) with the 2-mercaptopyridine ligand carried out in the same conditions. When the P–P ligand was c-dppen, dppe or dppp, the sole product were the corresponding $[Ru(pyS)_2(P–P)]$ complexes. However, with dppm and dppb a different pattern of reactivity was found and the main product was identified as $[Ru(pyS)_2(NO)(\eta^1\text{-P–PO})]PF_6$. In this sense, it is clear that the reactivity was controlled by the chain length between the phosphorus of diphosphines, in such a way that the small bite angle of the dppm ligand (≈72°) results in a ring strain which is eased by ready dissociation of one of the P atoms from the Ru center in the presence of the 'pyS^{-}' ligand. For the dppb complex, the explanation is the big bite angle (>90°) of this ligand, leaving the phosphorus atoms more susceptible to break its bond with the Ru center.

Supplementary data

CCDC 725472 and 725473 contain the supplementary crystallographic data for **1** and **5**, respectively. These data can be obtained free of charge via http://www.ccdc.cam.ac.uk/conts/retrieving.html, or from the Cambridge Crystallographic Data Centre, 12 Union Road, Cambridge CB2 1EZ, UK; fax: (+44) 1223-336-033; or e-mail: deposit@ccdc.cam.ac.uk

Acknowledgements

We thank FAPESP, CNPq, CAPES and FINEP for financial support.

References

[1] L.J. Ignarro, Nitric Oxide: Biology and Pathobiology, 1st ed., Academic Press, San Diego, 2000.
[2] M.J. Clarke, Coord. Chem. Rev. 232 (2002) 69–93.
[3] R. Eisenberg, C.D. Meyer, Acc. Chem. Res. 8 (1975) 26–34.
[4] M.J. Clarke, J.B. Gaul, Struct. Bond. 81 (1993) 147–181.
[5] P.G. Zanichelli, A.M. Miotto, H.F.G. Estrela, F.R. Soares, D.M. Grassi-Kassisse, R.C. Spadari-Bratfisch, E.E. Castellano, F. Roncaroli, A.R. Parise, J.A. Olabe, A. de Brito, D.W. Franco, J. Inorg. Biochem. 98 (2004) 1921–1932.
[6] E. Tfouni, M. Krieger, B.R. McGarvey, D.W. Franco, Coord. Chem. Rev. 236 (2003) 57–69.
[7] S.P. Fricker, E. Slade, N.A. Powell, O.J. Vaughan, G.R. Henderson, B.A. Murrer, I.L. Megson, S.K. Bisland, F.W. Flitney, Brit. J. Pharmacol. 122 (1997) 1441–1449.
[8] F. Bottomley, P.S. White, M. Mukaida, K. Shimura, H. Kakihana, J. Chem. Soc., Dalton Trans. (1978) 2965–2969.
[9] J.C. Toledo, B.S.L. Neto, D.W. Franco, Coord. Chem. Rev. 249 (2005) 419–431.
[10] G. Von Poelhsitz, A.A. Batista, J. Ellena, E.E. Castellano, E.S. Lang, Inorg. Chem. Commun. 8 (2005) 805–808.
[11] A. Massey, Y.Z. Xu, P. Karran, Curr. Biol. 11 (2001) 1142–1146.
[12] R. Cini, G. Tamasi, S. Defazio, M. Corsini, P. Zanello, L. Messori, G. Marcon, F. Piccioli, P. Orioli, Inorg. Chem. 42 (2003) 8038–8052.
[13] C.K. Mirabelli, R.K. Johnson, C.M. Sung, L. Faucette, K. Muirhead, S.T. Crooke, Cancer Res. 45 (1985) 32–39.
[14] F.B. Nascimento, G. Von Poelhsitz, F.R. Pavan, D.N. Sato, C.Q.F. Leite, H.S. Selistre-de-Araújo, J. Ellena, E.E. Castellano, V.M. Deflon, A.A. Batista, J. Inorg. Biochem. 102 (2008) 1783–1789.
[15] E.S. Raper, Coord. Chem. Rev. 153 (1996) 199–255.
[16] P.D. Akrivos, Coord. Chem. Rev. 213 (2001) 181–210.
[17] A.A. Batista, C. Pereira, S.L. Queiroz, L.A.A. de Oliveira, R.H.D. Santos, M.T.D. Gambardella, Polyhedron 16 (1997) 927–931.
[18] L.R. Dinelli, A.A. Batista, K. Wohnrath, M.P. de Araujo, S.L. Queiroz, M.R. Bonfadini, G. Oliva, O.R. Nascimento, P.W. Cyr, K.S. MacFarlane, B.R. James, Inorg. Chem. 38 (1999) 5341–5345.
[19] G. Von Poelhsitz, M.P. de Araujo, L.A.A. de Oliveira, S.L. Queiroz, J. Ellena, E.E. Castellano, A.G. Ferreira, A.A. Batista, Polyhedron 21 (2002) 2221–2225.
[20] T.S. Lobana, R. Singh, Polyhedron 14 (1995) 907–912.
[21] Enraf-Nonius, Collect, Nonius BV, Delft, The Netherlands, 1997–2000.

[22] Z. Otwinowski, W. Minor, HKL Denzo and Scalepack, in: C.W. Carter Jr., R.M. Sweet (Eds.), Methods in Enzymology, vol. 276, Academic Press, New York, 1997, pp. 307–326.
[23] R.H. Blessing, Acta Crystallogr., Sect. A 51 (1995) 33–38.
[24] G.M. Sheldrick, SHELXS-97. Program for Crystal Structure Resolution, University of Göttingen, Göttingen, Germany, 1997.
[25] G.M. Sheldrick, SHELXL-97. Program for Crystal Structures Analysis, University of Göttingen, Göttingen, Germany, 1997.
[26] L.J. Farrugia, J. Appl. Crystallogr. 30 (1997) 565.
[27] G. Von Poelhsitz, A.A. Batista, E.E. Castellano, J. Ellena, Inorg. Chem. Commun. 9 (2006) 773–776.
[28] G. Von Poelhsitz, B.L. Rodrigues, A.A. Batista, Acta Crystallogr., Sect. C 62 (2006) M424–M427.
[29] E.R.T. Tiekink, T.S. Lobana, R. Singh, J. Crystallogr. Spec. Res. 21 (1991) 205–208.
[30] J.R. Dilworth, Y.F. Zheng, S.F. Lu, Q.J. Wu, Trans. Metal Chem. 17 (1992) 364–368.
[31] C.A. Grapperhaus, M.Y. Darensbourg, Acc. Chem. Res. 31 (1998) 451–459.
[32] V.V. Grushin, Chem. Rev. 104 (2004) 1629–1662.
[33] J.D. Curry, R.J. Jandacek, J. Chem. Soc., Dalton Trans. (1972) 1120–1123.
[34] B.R. Penfold, Acta Crystallogr. 6 (1953) 707–713.
[35] M.M. Muir, S.I. Cuadrado, J.A. Muir, Acta Crystallogr., Sect. C 45 (1989) 1420–1422.
[36] T.S. Lobana, R. Verma, R. Singh, A. Castineiras, Trans. Metal Chem. 23 (1998) 25–28.
[37] G.B. Richter-Addo, P. Legzdins, Metal Nitrosyls, Oxford University Press, New York, 1992.
[38] T.S. Lobana, R. Verma, A. Castineiras, Polyhedron 17 (1998) 3753–3758.
[39] B.J. Coe, S.J. Glenwright, Coord. Chem. Rev. 203 (2000) 5–80.
[40] P.G. Douglas, R.D. Feltham, J. Am. Chem. Soc. 94 (1972) 5254–5258.
[41] R. Martos-Calvente, V.A.D. O'Shea, J.M. Campos-Martin, J.L.G. Fierro, J. Phys. Chem. A 107 (2003) 7490–7495.
[42] J.H. Enemark, R.D. Feltham, Coord. Chem. Rev. 13 (1974) 339–406.
[43] D.M.P. Mingos, D.J. Sherman, Adv. Inorg. Chem. 34 (1989) 293–377.
[44] M.I. Bruce, B.W. Skelton, A.H. White, N.N. Zaitseva, J. Organometal. Chem. 650 (2002) 141–150.
[45] P.W. Cyr, S.J. Rettig, B.O. Patrick, B.R. James, Organometallics 21 (2002) 4672–4679.
[46] R.W. Callahan, T.J. Meyer, Inorg. Chem. 16 (1977) 574–581.
[47] R.C.L. Zampieri, G. Von Poelhsitz, A.A. Batista, O.R. Nascimento, J. Ellena, E.E. Castellano, J. Inorg. Biochem. 92 (2002) 82–88.
[48] L.F. Szczepura, K.J. Takeuchi, Inorg. Chem. 29 (1990) 1772–1777.
[49] G. Exarchos, S.D. Robinson, J.W. Steed, Polyhedron 19 (2000) 1511–1517.
[50] J.C. Briggs, C.A. McAuliffe, G. Dyer, J. Chem. Soc., Dalton Trans. (1984) 423–427.
[51] O. Sigouin, A.L. Beauchamp, Inorg. Chim. Acta 358 (2005) 4489–4496.